Experimental investigation of full-scale post-tensioned composite AASHTO beams prestressed with carbon-fiber-reinforced polymer cables

Mahmoud R. Manaa, Abdeldjelil Belarbi, Bora Gencturk, and Mina Dawood

- This article reports on an investigation of the flexural behavior of five 39.5 ft long (12 m) post-tensioned beams with 0.76 in. diameter (19 mm) prestressing carbon-fiber-reinforced polymer (CFRP) cables under flexural monotonic and fatigue loading.
- At the ultimate load, the beams with unbonded cables showed greater deformation compared with the counterparts with bonded cables; however, the flexural capacity of the unbonded beams was lower.
- Different analytical models for estimating the flexural capacity of the beams were assessed against the experimental results to determine the applicability of these models to full-scale CFRP post-tensioned beams.

Post-tensioning is effectively used for new construction, rehabilitation, repair, and retrofitting of concrete structures. Typically, high-strength steel cables are the main type of reinforcement in prestressed concrete components. However, steel corrosion is a problem for structures exposed to chloride salts. Deteriorating structures require annual inspection, rehabilitation, and, in many cases, early replacement. Seven-wire steel cables are commonly used for concrete prestressing applications and are usually stressed to a high level exceeding 60% of the ultimate capacity. Therefore, losing a small area of prestressing strand to corrosion could lead to a substantial loss in strength.

In post-tensioned concrete structures, if the prestressing steel ducts are left ungrouted, the tendons could be exposed to water intrusion and atmospheric conditions leading to corrosion. Even when the prestressing steel is grouted, voids or cracks can lead to corrosion. Rigid grout is susceptible to cracking and water penetration, whereas the use of flexible grout involves practical challenges that currently limit its widespread adoption.

Corrosion-free reinforcement with mechanical properties similar to those of prestressing steel has been a research subject for the last three decades. The main topic of this research is the use of fiber-reinforced polymers (FRPs) as alternate, nonmetallic types of prestressing reinforcement. Among FRPs, carbon-fiber-reinforced polymers (CFRPs) are the most suitable option because they have a greater tensile strength and stiffness than other types of FRP. CFRPs have

been used in prestressing applications and have proved to be a viable alternative to steel strands, especially in aggressive environments where corrosion resistance is essential.[1]

Test results consistently indicate that while the overall behavior of CFRP-prestressed and steel-prestressed concrete beams are similar, several significant differences must be considered. These differences are primarily associated with the linear-elastic nature of the CFRP reinforcement. The load-deflection curve of a steel-prestressed concrete beam exhibits three stages, which reflect the elastic (before and after cracking) and inelastic properties. However, when CFRP is used for prestressing, the concrete beam exhibits only two stages: before cracking and after cracking up to the ultimate load. Because the modulus of elasticity of CFRP is low compared with that of steel, the curvatures and deflections induced in CFRP are larger than those induced in steel under the same level of flexural loading.[2] The deformation of CFRP-prestressed concrete beams at the point of rupture of CFRP tendons is smaller than that of the steel-prestressed concrete beams due to strain hardening in steel.[3]

As explained in the literature review section, below, a limited number of studies investigated the behavior of full-scale post-tensioned beams with unbonded prestressing CFRP. Previous research showed that under fatigue loading, failure in these types of beams typically occurs at the anchorage-tendon assembly, which leads to a premature failure of the system. Recently, there have been advancements in the tendon-anchor assembly design, therfore the performance of the assembly when used in full-scale beams with straight or draped profile configurations is investigated in this paper. In addition, the accuracy of the design guidelines to determine the ultimate flexural capacity of CFRP post-tensioned beams was evaluated. This area of investigation is important, especially for unbonded post-tensioning, because no unified approach has been established for estimating the tendon stress at ultimate load.

Literature review and previous experimental studies

Flexural behavior

The flexural behavior of post-tensioned beams with unbonded CFRP tendons has not been studied as extensively as that of prestressed beams with bonded CFRP tendons. Unbonded post-tensioned beams deform more than bonded post-tensioned beams as the force is transferred to the tendons through the anchorages. However, the load-carrying capacity of unbonded post-tensioned beams is generally less than that of bonded beams. Moreover, a few wide cracks are formed in unbonded cases while narrow cracks in bonded cases are distributed throughout the beam length.[4] Auxiliary (supplementary) bonded, unstressed reinforcement is added to the unbonded post-tensioned beams to control crack widths. The failure of unbonded post-tensioned beams is generally attributed to concrete crushing, even if the prestressing reinforcement levels are less than the balanced ratio of the corresponding bonded post-tensioned concrete beams.[5] The unbonded tendons lead to the release of stresses at critical sections, and, compared with the bonded tendons, they lower the average stress (and hence the load) along the tendon's length. As a result, the ultimate strength of beams with bonded tendons is greater than that of the unbonded counterparts regardless of the tendon type (steel or CFRP).

Several experimental studies have investigated the internal applications of unbonded prestressing CFRP tendons in beams. Most of these studies had beam lengths ranging from 6.6 to 10.5 ft (2.0 to 3.20 m), with beam depths ranging from 6 to 16 in. (150 to 410 mm) The results showed that unbonded beams have an energy absorption prior to failure comparable to that of the steel counterparts.[4,6-10] Heo et al.[10] reported that concrete crushing always occurred at the ultimate load regardless of the type of auxiliary (unstressed) reinforcement (CFRP or steel) used. Maissen and De Smet[8] showed that continuous beams with unbonded prestressing CFRP tendons provided the same level of deformability as those with steel tendons. However, once the cable ruptures at the hinge forming above the intermediate supports, the beams prestressed with bonded CFRP tendons did not redistribute the moment as there was no reserve capacity.

Previous tests[3,11,12] have demonstrated that the level of prestressing, the prestressing reinforcement ratio, and the presence of unstressed reinforcement in the tensile zone have significant effects on the deformation of beams prestressed with bonded CFRP tendons. Selvachandran et al.[13] tested four bonded post-tensioned beams with CFRP bars designed to fail in tension under a simply supported condition. The results indicated that the greater the prestressing force was, the greater the cracking moment was. In addition, the prestressing force did not affect the ultimate strength of the components, despite their deformability. Grace et al.[14] comprehensively investigated the design, construction, and monitoring of the longest highway bridge span prestressed with a CFRP system in the United States. They experimentally studied possible failure modes of the CFRP-prestressed concrete beams and discussed design, construction, and field monitoring. The results from experimental, analytical, and field data showed that the bridge performed as expected under service loads with a high reserved capacity.

Fatigue behavior

Existing research and design guidelines suggest that flexural fatigue is not expected to be a governing limit state in the design of CFRP-prestressed concrete beams because under service loading conditions, the beams are expected to remain uncracked. However, accidental overloading of the beam could lead to cracking. The repeated opening and closing of the cracks due to overloading could result in a reduced fatigue life of the CFRP tendons. In previous studies,[3,15,16] the beams were typically precracked before the start of the fatigue cycles. The results showed that fatigue had no significant effect on the load-carrying capacity and stiffness of the beams even under extreme

environmental conditions. For unbonded post-tensioned beams, there is no concentration of stresses at the cracks because the stresses are averaged out along the tendon length. However, the unbonded tendons experience stress concentrations at the anchor locations, which may lead to their premature failure. Braimah et al.[17] tested five unbonded post-tensioned concrete beams with bonded non-prestressed GFRP bars under flexural fatigue loading. It was observed that the failure of the prestressed CFRP bars at the anchors initiated failure of the post-tensioned beams, whereas the non-prestressed GFRP bars did not show any failure during the fatigue loading.

External post-tensioning

An alternative approach for strengthening existing structures is the unbonded post-tensioning of beams using tendons placed outside the cross section of the member. Mutsuyoshi and Machida,[18] Grace and Abdel-Sayed,[19] Elrefai et al.,[20] Du and Au,[21] and Ghallab[22] investigated the flexural behavior of beams with external prestressing CFRP and found that the behavior of these beams was similar to that of beams prestressed with steel tendons. Grace et al.[12] investigated the behavior of multispan continuous CFRP-prestressed concrete bridges with external longitudinal post-tensioning using draped tendons and bonded transverse post-tensioning. They reported that a progressive failure of the CFRP tendons was observed at the ultimate load stage.

Deformability

Beams that are prestressed with CFRP do not exhibit ductility, and the behavior under load is bilinear and elastic up to failure. Traditional definitions of ductility relate some measure of a beam's deformation at ultimate (strain, curvature, deformation, absorbed energy, etc.) to the same measure of its deformation when the reinforcement yields. Because CFRP reinforcement does not exhibit yielding, ductility cannot be determined in the traditional sense. Therefore, deformability has been proposed as a measure of the performance of beams reinforced or prestressed with brittle reinforcements.[2,23,24] Generally, definitions of deformability relate some measure of a beam's deformation at ultimate to its deformation under service loads. To predict deformability, energy-based models are insensitive to the magnitude of the ultimate deformation of the component. This assumption may be appropriate for applications where energy dissipation is a primary design consideration (for example, seismic design). For concrete components with brittle reinforcement, Naaman and Jeong[25] developed Eq. (1), referred to as the ductility index μ_{en}, which is based on energy parameters assuming that the behavior of prestressed concrete beams is fully elastoplastic. The ductility index is also applicable to CFRP-prestressed concrete beams.

$$\mu_{en} = 0.5\left(\frac{E_{tot}}{E_{ela}}\right) \quad (1)$$

where

E_{tot} = total energy under the load-deflection curve

E_{ela} = elastic energy, which is a part of the total energy

For bridge beams where energy dissipation is not a consideration, deformability may be a more suitable parameter to evaluate safety and performance. Studies[26,27] show that the inclusion of distinct deformation parameters, such as deflection at ultimate and deflection at cracking, in the deformability index provides a reasonable measure of the performance of the CFRP-prestressed beams. Abdelrahman et al.[26] proposed a model for the deformability of CFRP-prestressed beams μ as the ratio of the actual deformation at the ultimate state to the equivalent deformation of the uncracked section at the same load level as Eq. (2).

$$\mu = \frac{\Delta_u}{\Delta_\ell} \quad (2)$$

where

Δ_u = deflection at ultimate load

Δ_ℓ = equivalent deflection of an uncracked section at the same ultimate load

Experimental program

The work presented in this paper was completed as a part of an NCHRP project.[28] An article about the work on pretensioned beams was recently published in the *PCI Journal*.[29]

Test matrix

Five full-scale CFRP-prestressed concrete bridge beams were constructed and tested under flexural loading. Two different loading conditions were considered: monotonic flexure and flexural fatigue. **Table 1** shows the test matrix of the full-scale beams included in the experimental program. Two beams were grouted to represent the fully bonded case, whereas the other three beams were left unbonded. Three beams were tested under static loading up to failure. The other two beams were tested under four-point bending flexural fatigue loading. A draped tendon profile was used in the bonded beams, and both straight and draped tendon profiles were studied in the unbonded beams. Specimen designations to describe each specimen were assigned:

- CPouDF = CFRP post-tensioned beam with unbonded draped cables subjected to the flexural fatigue loading condition
- CPouSF = CFRP post-tensioned beam with unbonded straight cables subjected to the flexural fatigue loading condition
- CPouSM = CFRP post-tensioned beam with unbonded straight cables subjected to the monotonic flexure loading condition
- CPoDM#01 = CFRP post-tensioned beam with bonded

Table 1. Test matrix of beams prestressed with carbon-fiber-reinforced polymer (CFRP) cables

Beam identifier	Type of prestressing CFRP	Type of prestressing	Prestressing CFRP profile	Type of loading	Repetitions
CPoDM#01	Cable	Post-tensioned bonded (Po)	Draped (D)	Monotonic (M)	2
CPoDM#02					
CPouSF		Post-tensioned un-bonded (Pou)	Straight (S)	Flexural fatigue (F)	1
CPouSM				Monotonic (M)	1
CPouDF			Draped (D)	Flexural fatigue (F)	1

Note: CPouDF = CFRP post-tensioned beam with unbonded draped cables subjected to the flexural fatigue loading condition; CPouSF = CFRP post-tensioned beam with unbonded straight cables subjected to the flexural fatigue loading condition; CPouSM = CFRP post-tensioned beam with unbonded straight cables subjected to the monotonic flexure loading condition; CPoDM#01 = CFRP post-tensioned beam with bonded draped cables subjected to the monotonic flexure loading condition (first specimen of this type); CPoDM#02 = CFRP post-tensioned beam with bonded draped cables subjected to the monotonic flexure loading condition (second specimen of this type).

draped cables subjected to the monotonic flexure loading condition (first specimen of this type)

- CPoDM#02 = CFRP post-tensioned beam with bonded draped cables subjected to the monotonic flexure loading condition (second specimen of this type)

Material properties

The precast concrete used in this research had a 28-day target compressive strength of 9000 psi (62 MPa) for the deck and the girder concrete. During each casting, standard cylinders (4 in. [100 mm] diameter and 8 in. [200 mm] in height) were cast. according to ASTM C31, *Standard Practice for Making and Curing Concrete Test Specimens in the Field*.[30] These cylinders were tested according to ASTM C39, *Standard Test Method for Compressive Strength of Cylindrical Concrete Specimens*,[31] to determine the concrete strength for each beam.

The prestressing CFRP systems (including anchorages) were acquired from one manufacturer. A 0.76-in.-diameter (19-mm) seven-wire cable with a 0.289 in.^{2} (186 mm^2) effective area was used. The manufacturer reported that the design tensile strength was 377 ksi (2600 MPa), the elastic modulus was 23,200 ksi (160,000 MPa), and the maximum longitudinal strain was 1.6%. Ten uniaxial tensile tests were conducted on the prestressing CFRP cables in accordance with ASTM D7205-06, *Standard Test Method for Tensile Properties of Fiber Reinforced Polymer Matrix Composite Bars*.[32] The cables were instrumented with a noncontact optical extensometer for the measurement of elongations. In addition, five of the test specimens were instrumented with a contact extensometer and strain gauges. The strain gauges were installed on one of the individual wires along the axis of the cable. The contact extensometer was removed when the tensile load on the specimen reached 60% of the expected capacity. The minimum and maximum tensile strengths were recorded as 106.0 and 110.7 kip (471.5 and 492.4 kN), respectively. The mean tensile strength was calculated as 109.1 kip (485.3), and the standard deviation was found to be 1.3 kip (5.8 kN). Accordingly, the guaranteed tensile strength of the prestressing CFRP cables, defined as the mean tensile strength minus three standard deviations, was 105.2 kip (467.9 kN). The characteristic value was calculated as 102 kip (454 kN) according to ASTM D7290, *Standard Practice for Evaluating Material Property Characteristic Values for Polymeric Composites for Civil Engineering Structural Application*.[33]

A high-strength, nonshrink cementitious grout was used for grouting all the prestressing CFRP cables of the two post-tensioned beams to create the bonded cases. The grout compressive strength at 28 days was 15,000 psi (103 MPa). A corrugated polypropylene duct was used for the construction of all post-tensioned beams. The inner diameter of the duct was 2 in. (50 mm). The duct size was controlled by the preattached sockets on the CFRP cable, rather than the cable diameter. The cables were provided by the manufacturer with the preattached sockets.

Specimen design and fabrication

All beams were fabricated at a precast concrete plant. The beams were 39.5 ft (12.0 m) long and 28 in. (710 mm) deep with an AASHTO Type I cross-sectional geometry having a 36 in. (910 mm) wide, 8 in. (200 mm) thick composite cast-in-place concrete slab. **Figures 1** and **2** present the cross-sectional geometry of the test beams. The beam cross section and span were selected to result in a shear span-to-depth ratio *a*/*d* of approximately 7.0, which was sufficient to study the flexural behavior of such a system. All the beams were designed to prevent premature shear failures and ensure a flexural failure. **Figure 3** shows the typical reinforcement details for the beam with draped cables. Other beams had similar reinforcing details.

The preattached anchorage system consisted of a threaded stainless steel socket. The steel socket was 16.5 in. (419 mm) long with threads on both the outer and the inner surfaces. An expansive cementitious grout was used to fix the prestressing CFRP inside the socket, where the internal threads provided

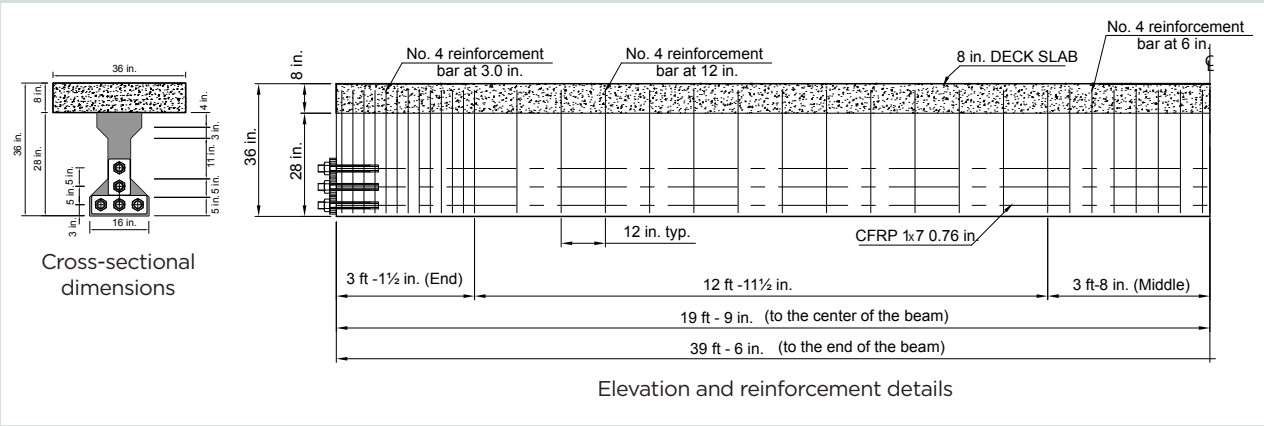

Figure 1. Typical details for full-scale post-tensioned concrete beams with straight cables. Note: CFRP = carbon-fiber-reinforced polymer. No. 4 = 13M. 1 in. = 25.4 mm; 1 ft = 0.305 m.

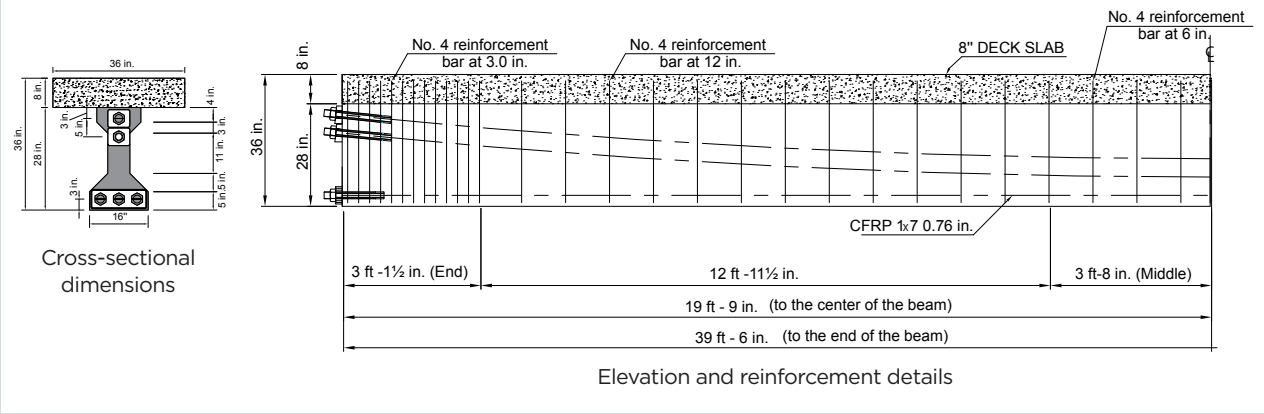

Figure 2. Typical details for full-scale post-tensioned concrete beams with straight and draped cables. Note: CFRP = carbon-fiber-reinforced polymer. 1 in. = 25.4 mm; 1 ft = 0.305 m.

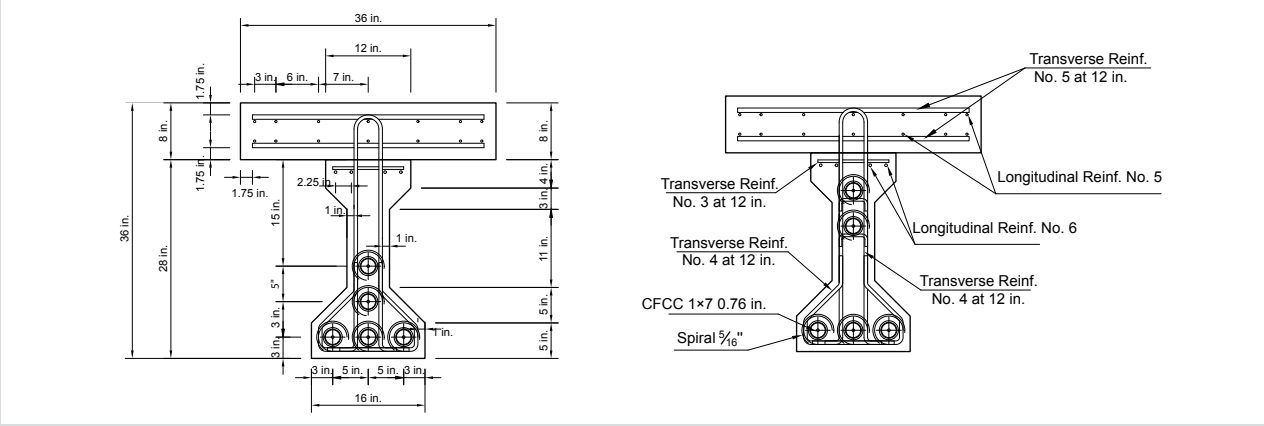

Figure 3. Typical reinforcement details for full-scale post-tensioned concrete beams with draped cables. Note: CFRP= carbon-fiber-reinforced polymer. No. 3 = 10 M; no. 4 = 13M; no. 5 = 16M; no. 6 = 19M. 1 in. = 25.4 mm.

additional resistance against the slippage of the prestressing CFRP. The cables were instrumented and inserted inside the ducts. Depending on the available lengths of the duct, couplers were used to connect two pieces of the same duct and heat-shrinkable tubular sleeves were used for sealing the connection. Both longitudinal and transverse steel were inserted around the ducts. After completing the reinforcement cages, the lifting points were added, and the steel forms were placed onto the casting bed to start casting.

For bonded post-tensioned beams, grouting saddles were attached to the ends and middle of each duct to provide inlet and outlet points. The ends of each duct were connected to a slip-on coupler because the available space between the duct and the socket was not sufficient to encapsulate the socket with grout and to allow the air to flow out freely. Two outlets and one inlet were installed on the ducts. The inlet was in the middle of the beam, and the outlets were at each end of the duct.

The post-tensioning was performed at the precasting plant immediately after the forms were removed and before the installation of the slab forms. The target jacking load in each of the CFRP cables was 60 kip (270 kN), the equivalent of 60% of the design breaking load provided by the manufacturer. The threaded stainless steel socket was anchored by a nut. The expected seating losses were minimum with insignificant slippage. In the field, measurements were conducted to determine the anchorage seating losses, and they were found to be less than 1.0% of the jacking force. The composite slab was cast immediately after the post-tensioning. After sufficient curing, the beams were transported to the structural testing laboratory.

Loading protocols

In the monotonic flexural testing, a seating load of 32 kip (140 kN) (approximately one-third of the cracking load) was applied to the beam to eliminate the initial slack of the load application system. The load was then released to 18.2 kip (81.0 kN) to finalize the seating, and the actual loading protocol was initiated. The beams were then tested in displacement control mode.

In most of the published literature,[17,20,26] beams reaching 2.3 million cycles were identified as "run-out" tests with an apparently infinite fatigue life. The two beams tested under fatigue loading reached the 2.3 million cycles and were tested monotonically to failure to evaluate their residual capacities. The fatigue loading was stopped intermittently, and a monotonic flexural test was conducted within the elastic range to evaluate stiffness degradation of the beams due to cyclic loading. The flexural fatigue testing procedure was performed as follows:

1. The beam was loaded monotonically until the first crack to simulate the accidental overload (**Fig. 4**).

2. The load was removed, returning the beam to its original position.

3. The beam was loaded from the lower limits of fatigue loading (13 kip (58 kN) or 20% of cracking load and 20 kip [89 kN] or 28% of cracking load for CPouSF and CPouDF, respectively) to the upper limits of fatigue loading (65 and 72 kip [290 and 320 kN], for CPouSF and CPouDF, respectively), which constituted the cracking load of the beams. The lower limits of the fatigue loading were calculated by subtracting the fatigue truck moment (using a girder distribution factor *GDF* = 1) from the cracking moment.

4. Every 500,000 cycles, the fatigue test was stopped, and the beams were tested twice under monotonic loading up to the upper fatigue limit. The applied load, vertical

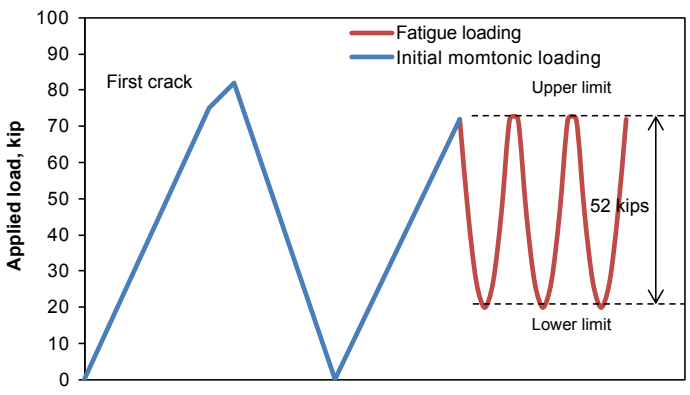

Loading protocol

Initial crack pattern

Figure 4. Loading protocol for flexural fatigue testing. Note: 1 kip = 4.448 kN.

deflections, prestressing tendon strains, and crack widths were measured.

5. The fatigue test was resumed until the next target number of cycles (1 million, 1.5 million, 2 million, and 2.3 million).

6. The beams were then loaded to failure under monotonic loading after reaching the target maximum number of cycles.

Instrumentation

All beams were instrumented with various types of sensors to monitor flexural behavior. Conventional load cells, linear variable differential transformers, string potentiometers, and strain gauges were used at different locations to measure the applied load, deformations, crack widths, and strains. In addition to conventional instrumentation, a noncontact measurement system was used to monitor the local and global behavior of the beams. Specifically, a three-dimensional (3-D) digital image correlation system and a 3-D point measurement system were used. Both systems were used, in addition to the conventional measuring devices, to measure the beam deformation. **Figure 5** shows the locations of both systems as well as conventional sensors used to measure the displacements.

Results

Fatigue loading

Both unbonded CFRP post-tensioned beams, CPouSF (straight cables) and CPouDF (draped cables), were tested under fatigue loading. Both beams survived the target fatigue cycles of 2.3 million, and they were then monotonically tested to failure. **Figure 6** shows the effect of fatigue loading on the stiffness of both beams. The change in the beams' stiffness was not significant when compared with the initial stiffness.

Monotonic loading

Figures 7 and **8** present the load-deflection curves from the monotonic tests of all five post-tensioned beams. As mentioned earlier, the parameters included in the experimental program were the bond condition, cable profile, and flexural loading type. The overall behavior of the beams was piece-wise linear with two distinct stiffnesses up to failure. The initial stiffness of the beam reduced after the crack opening and remained almost constant up to the ultimate load. Concrete crushing failure was observed at the ultimate load for all unbonded post-tensioned beams (Fig. 7), whereas the bonded beams failed due to the rupture of the prestressing CFRP cables (Fig. 8). All the unbonded post-tensioned beams except for CPouSF reached almost the same peak load level. CPouSF had a 10% less capacity compared with the similar CPouSM beam. This finding shows the effect of the fatigue loading cycles on the concrete strength. Additionally, the effect of having draped cables on the capacity was insignificant despite that the capacity of the beam with draped cables was slightly higher than the beams with straight cables. This higher capacity was a result of the higher effective prestressing forces in the beam with draped cables. Figure 8 shows the effect of the bond condition. The beams with bonded cables CPoDM#01 and CPoDM#02 showed an approximately 20% higher capacity than the similar unbonded beam CPouDF. Finally, the influence of the effective prestressing force is evident when the two bonded post-tensioned beams are compared, as the beam with a higher effective prestressing force showed a higher cracking load and less deflection despite having the same peak loads as the other beam.

The deflection profiles were obtained from the string potentiometers located along the beam length. **Figure 9** shows the deflection profiles for each post-tensioned beam at two stages of the experiments: the first stage was at 5 in. (130

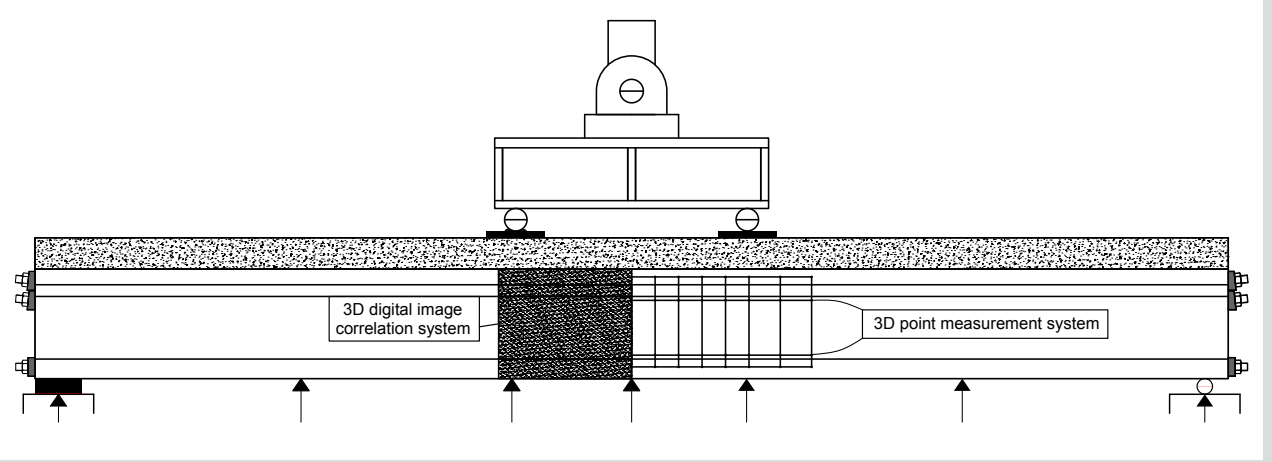

Figure 5. Locations of noncontact instrumentation and string potentiometers.

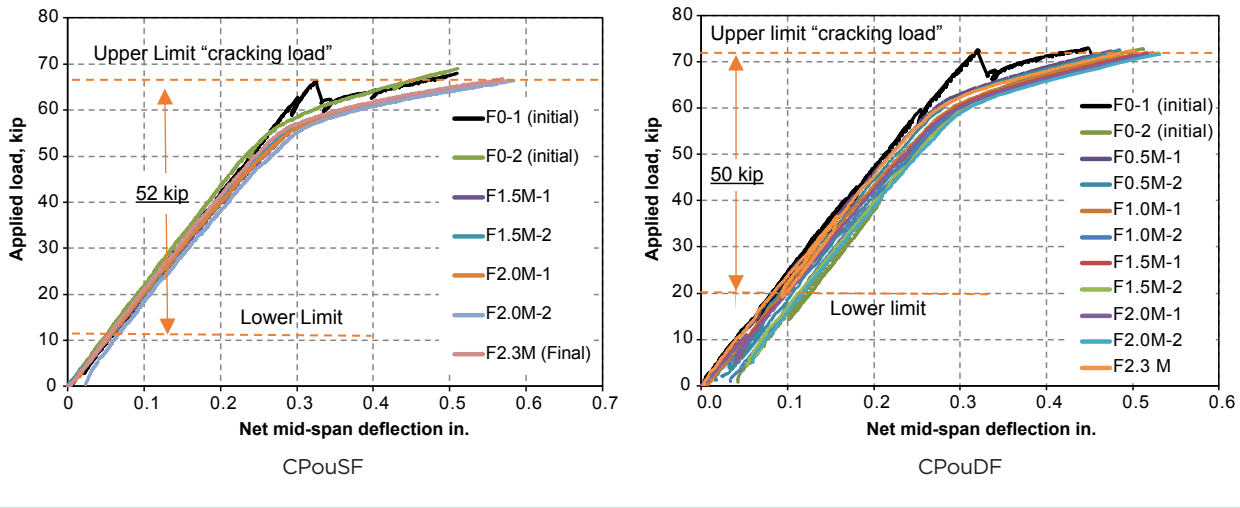

Figure 6. Load-deflection response of the post-tensioned concrete beams between the fatigue loading cycles. CFRP = carbon-fiber-reinforced polymer; CPouDF = CFRP post-tensioned beam with unbonded draped cables subjected to the flexural fatigue loading condition; CPouSF = CFRP post-tensioned beam with unbonded straight cables subjected to the flexural fatigue loading condition. 1 in. = 25.4 mm; 1 kip = 4.448 kN.

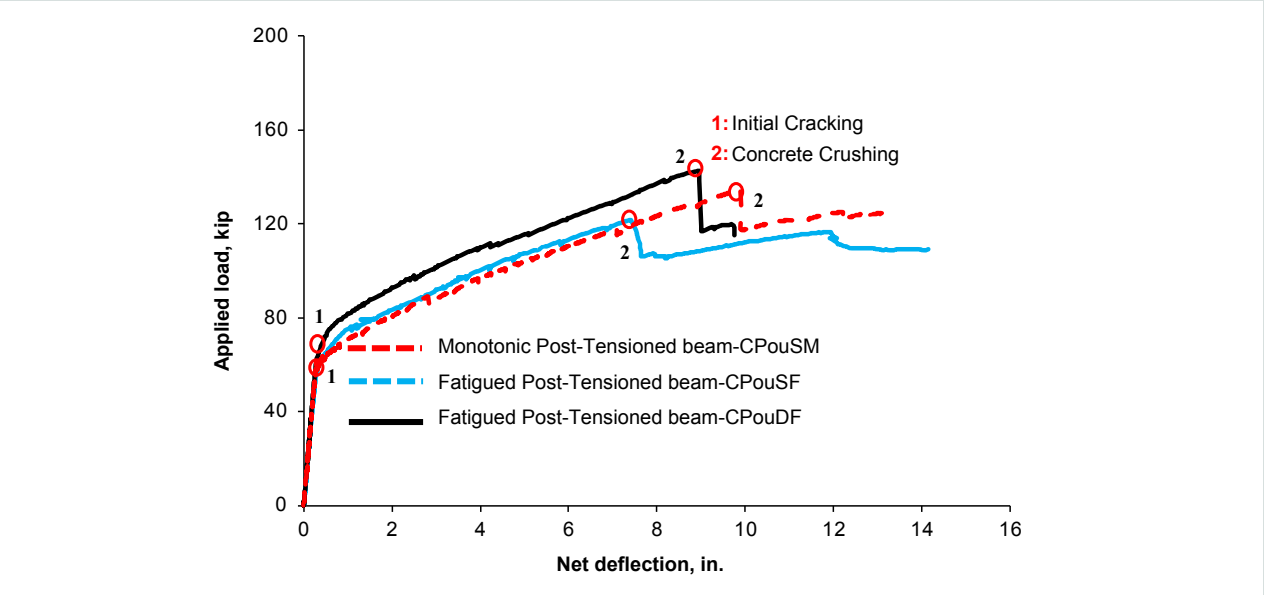

Figure 7. Load-deflection response for unbonded post-tensioned concrete beams with prestressing carbon-fiber-reinforced polymer (CFRP). Note: CPouDF = CFRP post-tensioned beam with unbonded draped cables subjected to the flexural fatigue loading condition; CPouSF = CFRP post-tensioned beam with unbonded straight cables subjected to the flexural fatigue loading condition; CPouSM = CFRP post-tensioned beam with unbonded straight cables subjected to the monotonic flexure loading condition. 1 in. = 25.4 mm; 1 kip = 4.448 kN.

mm) deflection at midspan, and the second was at peak load. The results showed a concentration of rotation at the constant moment region for all beams. When the net deflection equaled 5 in. (Fig. 9) at the midspan, the deflection profiles for unbonded and bonded beams were comparable, with a slight increase for the bonded beams at other locations. At the peak load (Fig. 9), the unbonded post-tensioned beams had a higher deflection, acting similar to a shallow tied arch, which was similar to the behavior of unbonded post-tensioned beams with prestressing steel.[32] The bonded post-tensioned beams maintained their deflected shape until the ultimate load.

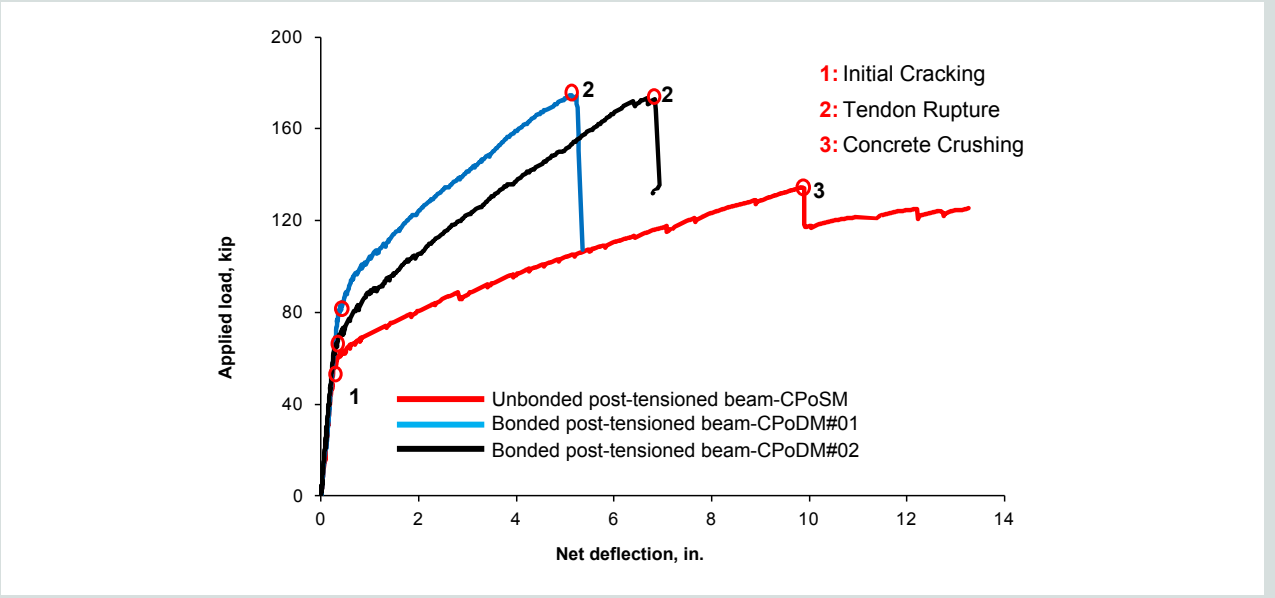

Figure 8. Load-deflection response for unbonded post-tensioned concrete beams with prestressing carbon-fiber-reinforced polymer (CFRP). Note: CPouSM = CFRP post-tensioned beam with unbonded straight cables subjected to the monotonic flexure loading condition; CPoDM#01 = CFRP post-tensioned beam with bonded draped cables subjected to the monotonic flexure loading condition (first specimen of this type); CPoDM#02 = CFRP post-tensioned beam with bonded draped cables subjected to the monotonic flexure loading condition (second specimen of this type). 1 in. = 25.4 mm; 1 kip = 4.448 kN.

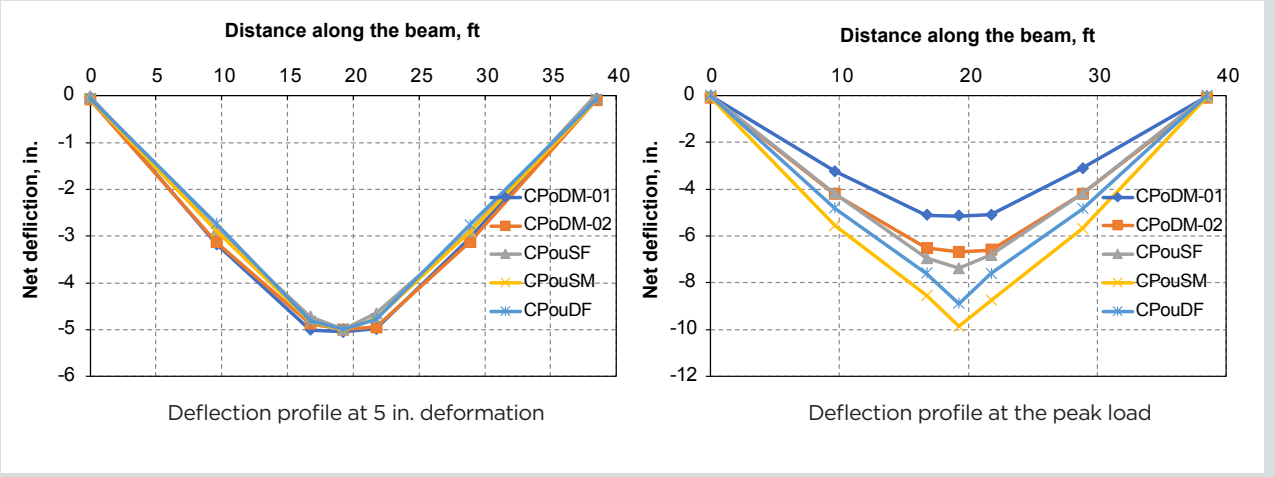

Figure 9. Deflection profiles of the carbon-fiber-reinforced polymer post-tensioned concrete beams. Note: CFRP = carbon-fiber-reinforced polymer; CPouDF = CFRP post-tensioned beam with unbonded draped cables subjected to the flexural fatigue loading condition; CPouSF = CFRP post-tensioned beam with unbonded straight cables subjected to the flexural fatigue loading condition; CPouSM = CFRP post-tensioned beam with unbonded straight cables subjected to the monotonic flexure loading condition; CPoDM#01 = CFRP post-tensioned beam with bonded draped cables subjected to the monotonic flexure loading condition (first specimen of this type); CPoDM#02 = CFRP post-tensioned beam with bonded draped cables subjected to the monotonic flexure loading condition (second specimen of this type). 1 in. = 25.4 mm; 1 ft = 0.305 m.

Table 2 shows the deformability indexes calculated from the two different methods, the energy-based model proposed by Naaman and Jeong[25] and the deformation-based model proposed by Abdelrahman et al.[26] A drawback of the energy method is that it does not differentiate between the unbonded and bonded beams. When this method was used, the bonded beams with different prestressing ratios had the same deformability index, which is questionable. When the deformation-based method was used, the deformability index was higher for the unbonded beams than for the bonded beams. In addition, the bonded beam with a higher prestressing ratio (CPoDM#1) showed a lower deformability compared with the one with a lower prestressing ratio (CPoDM#2).

Table 2. Summary of the test results of the full-scale beams

Beam identifier	Cracking load, kip	Ultimate		Failure mode	Predicted load capacity, kip		Deformability index	
		Load, kip	Deflection, in.		ACI 440-R	AASHTO LRFD specifications	Abdelrahman et al.	Naaman and Jeong
CPouSM	61	135	9.9	Concrete crushing	144.7	104.2	14.4	1.21
CPouSF	65	122	7.4				10.8	1.33
CPouDF	72	143	8.9				12.4	1.26
CPoDM#01	81.4	175	5.2	Cable rupture	151.6	n/a	6.4	1.23
CPoDM#02	62.8	174	6.7				9.5	1.26

Note: CPouDF = CFRP post-tensioned beam with unbonded draped cables subjected to the flexural fatigue loading condition; CPouSF = CFRP post-tensioned beam with unbonded straight cables subjected to the flexural fatigue loading condition; CPouSM = CFRP post-tensioned beam with unbonded straight cables subjected to the monotonic flexure loading condition; CPoDM#01 = CFRP post-tensioned beam with bonded draped cables subjected to the monotonic flexure loading condition (first specimen of this type); CPoDM#02 = CFRP post-tensioned beam with bonded draped cables subjected to the monotonic flexure loading condition (second specimen of this type); n/a = not applicable. 1 in. = 25.4 mm; 1 kip = 4.448 kN; 1 ksi = 6.895 MPa.

During the experiments, the unbonded cable force was contiously measured and recorded via a load cell attached to the dead end of a selected cable in each beam while the strain of the bonded cables was recorded through preattached strain gauges. Two of the unbonded cables of beams CPouDF and CPouSM were equipped with the load cells. **Figure 10** compares the increase in the cable force with the increasing applied load for both beams (straight and draped). At the same applied load level or displacement, the bonded cables experienced a greater increase in the cable force compared with the unbonded cables. The rate of increase in the unbonded cable load at the bottom was the same for CPouSM and CPouDF. Additionally, in the top cable, which was straight in CPouSM and draped in CPouDF, the rate of increase was similar. The location of the cable significantly affected the cable force. The force in the bottom cable was almost 60% greater than that in the top cables.

The unbonded post-tensioned beams failed due to concrete crushing. Once the beams reached the ultimate point, the load dropped with a reserve in the load-carrying capacity. In contrast, the bonded post-tensioned beams failed due to the rupture of the CFRP cables. **Figure 11** shows the failure modes of the bonded and unbonded post-tensioned beams.

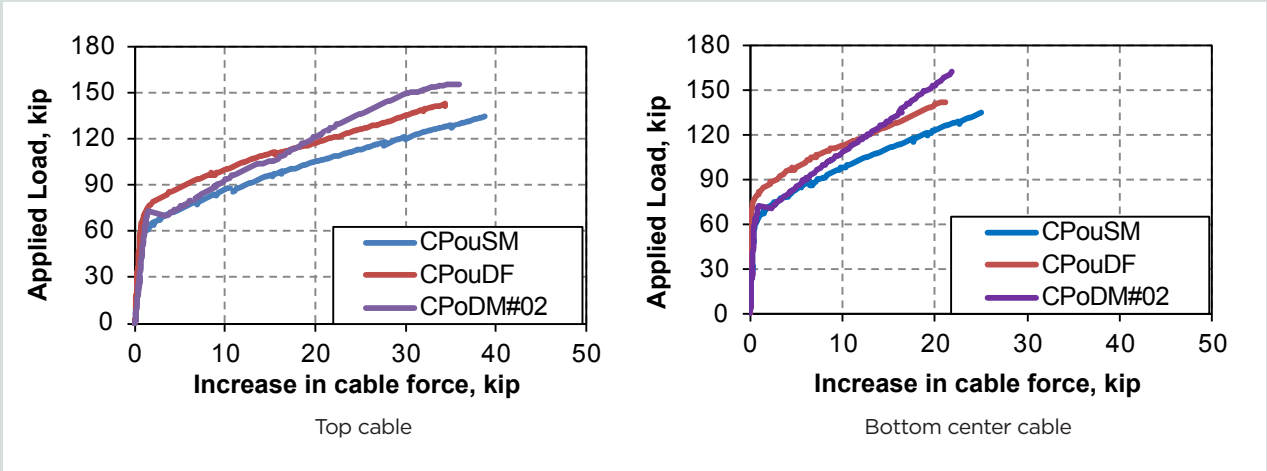

Figure 10. Applied load versus increase in cable force for various cables of post-tensioned concrete beams. Note: CPouDF = CFRP post-tensioned beam with unbonded draped cables subjected to the flexural fatigue loading condition; CPouSM = CFRP post-tensioned beam with unbonded straight cables subjected to the monotonic flexure loading condition; CPoDM#02 = CFRP post-tensioned beam with bonded draped cables subjected to the monotonic flexure loading condition (second specimen of this type). 1 kip = 4.448 kN.

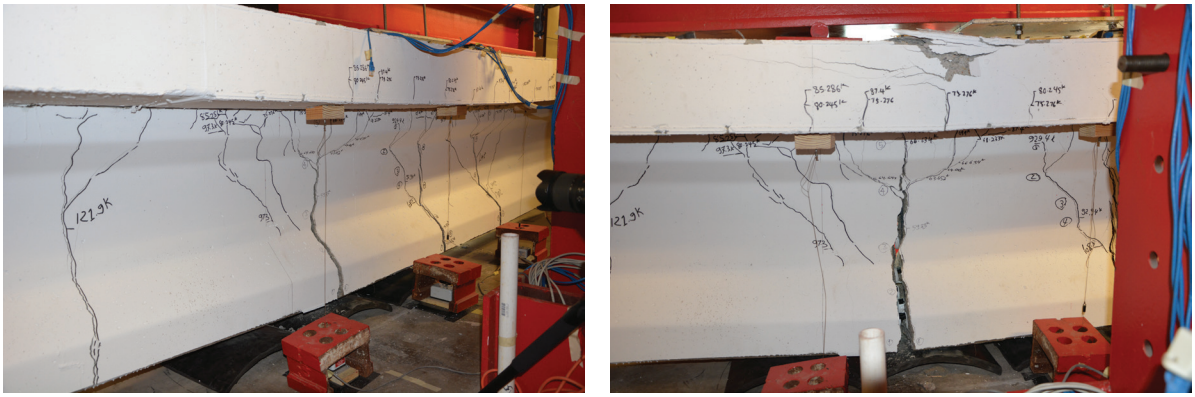

CPouSM

CPouSF

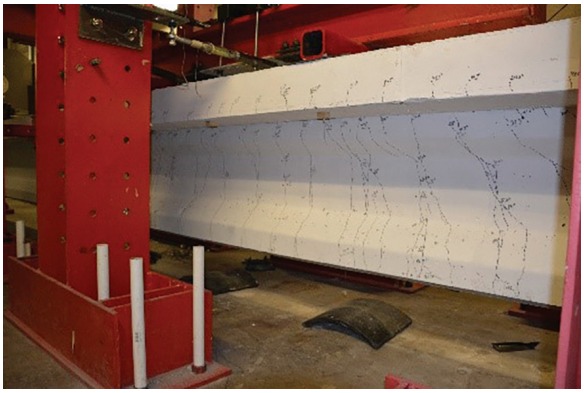

CPoDM#02

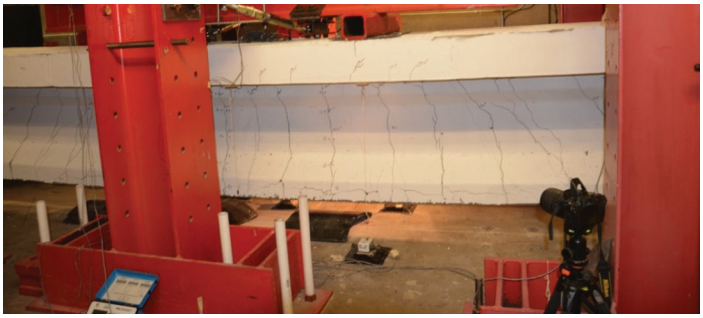

CPoDM#01

CPouDM

Figure 11. Failure modes of post-tensioned concrete beams with prestressing carbon-fiber-reinforced polymer. Note: CFRP = carbon-fiber-reinforced polymer; CPouDF = CFRP post-tensioned beam with unbonded draped cables subjected to the flexural fatigue loading condition; CPouSF = CFRP post-tensioned beam with unbonded straight cables subjected to the flexural fatigue loading condition; CPouSM = CFRP post-tensioned beam with unbonded straight cables subjected to the monotonic flexure loading condition; CPoDM#01 = CFRP post-tensioned beam with bonded draped cables subjected to the monotonic flexure loading condition (first specimen of this type); CPoDM#02 = CFRP post-tensioned beam with bonded draped cables subjected to the monotonic flexure loading condition (second specimen of this type).

The monotonic tests of the full-scale beams were done in stages to track crack propagation and allow for crack-width measurements. In the unbonded post-tensioned beams, a few concentrated wide cracks were observed, which branched into smaller cracks under additional loading. This behavior was like the behavior exhibited by unbonded beams post-tensioned with prestressing steel as documented by Mattock et al.[34] However, for bonded prestressed beams, the cracks were spread over approximately a quarter of the length from the center of the beam on each side.

Figure 12 compares the maximum crack-width measurement versus applied loads for both bonded and unbonded post-tensioned beams. The crack width in the unbonded beams was seven times larger than that of the bonded beams. **Figure 13** shows a schematic crack distribution for the full-scale post-tensioned beams at the ultimate load.

Evaluation of analytical models for moment capacity

Bonded post-tensioned beams

An approach like that set forth in the American Concrete Institute's *Prestressing Concrete Structures with FRP*

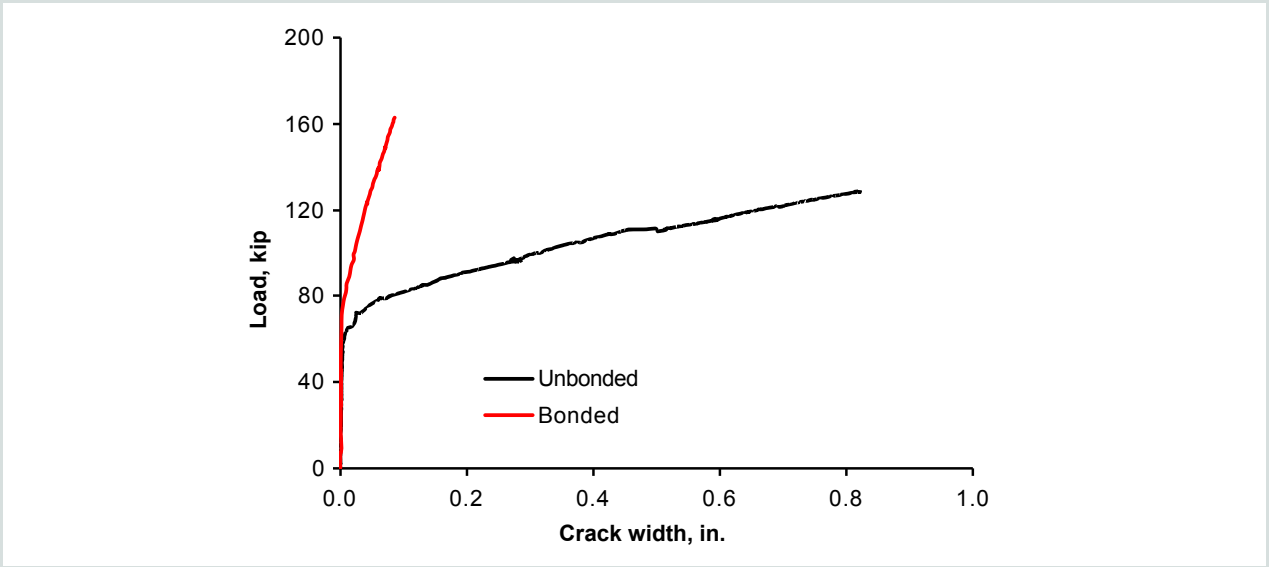

Figure 12. Maximum crack width for two post-tensioned concrete beams obtained from the digital image correlation system or point tracking system against the applied load. Note: 1 in. = 25.4 mm; 1 kip = 4.448 kN.

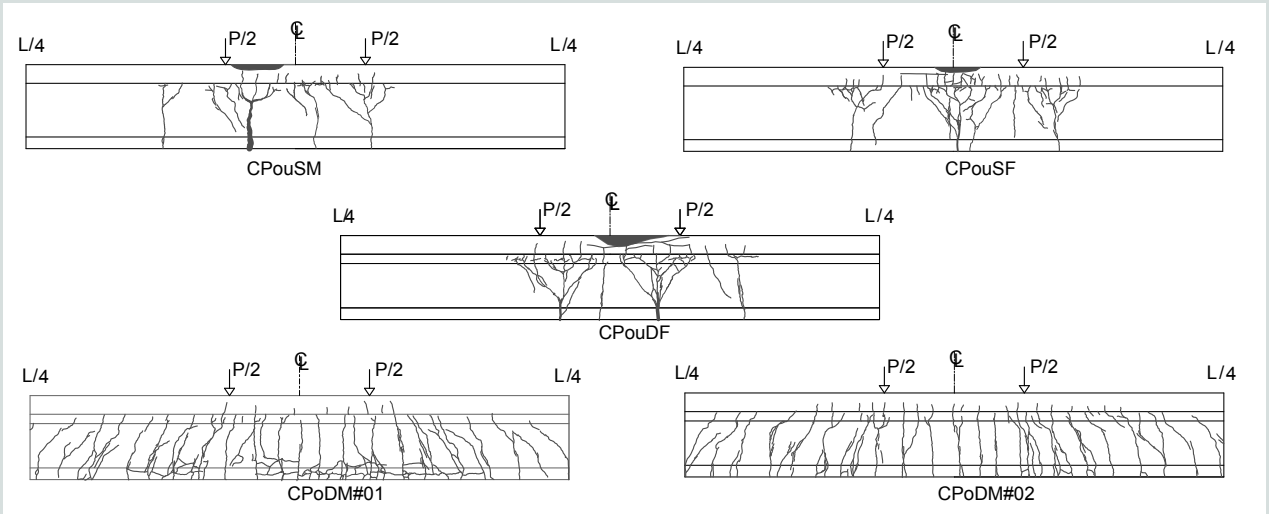

Figure 13. Crack patterns in the monotonic tests of the full-scale carbon-fiber-reinforced polymer (CFRP)–prestressed concrete beams at ultimate load. Note: CPouDF = CFRP post-tensioned beam with unbonded draped cables subjected to the flexural fatigue loading condition; CPouSF = CFRP post-tensioned beam with unbonded straight cables subjected to the flexural fatigue loading condition; CPouSM = CFRP post-tensioned beam with unbonded straight cables subjected to the monotonic flexure loading condition; CPoDM#01 = CFRP post-tensioned beam with bonded draped cables subjected to the monotonic flexure loading condition (first specimen of this type); CPoDM#02 = CFRP post-tensioned beam with bonded draped cables subjected to the monotonic flexure loading condition (second specimen of this type); L = length of the tendon between the anchorages; P = load.

Tendons (ACI 440-4R)[2] was used to calculate the flexural capacity of the beams. The calculation started by assuming a location for the neutral axis and comparing it with the one obtained from the balanced condition to determine the failure mode. For sections failing by concrete crushing, the ultimate compressive strain was assumed to equal 0.003. The tendons located at the extreme tension layer were assumed to reach the rupture strength. The forces in the other tendons and concrete strains were obtained accordingly based on strain compatibility. For both cases, the rectangular stress block parameters α_1 (multiplier for concrete strength) and β_1(multiplier for the neutral axis depth) were calculated according to the American Association of State Highway and Transportation Officials' AASHTO LRFD Bridge Design Specifications.[35]

Unbonded post-tensioned beams

Two models were used to calculate the load in the unbonded cables at the ultimate point. The first model, adopted by ACI 440-4R, is based on the work done by Naaman and Alkhairi[36] and uses the strain reduction approach. The second model is that in AASHTO LRFD specifications, which is based on the work of MacGregor[37] for prestressing steel and uses the failure mechanism approach. These models were originally developed for unbonded prestressing steel tendons with the assumptions that the steel will not reach the nonlinear stage and that the elastic modulus of steel can be used to predict the stress in the tendons.[38,39] Given the linear-elastic nature of CFRP, these models can be used to predict the load in unbonded tendons at the ultimate point according to the procedures described herein.

ACI 440-4R recommends a model for calculating the load in unbonded CFRP tendons. The total force in the unbonded tendon f_{pf} can be calcuated by Eq. (3).

$$f_{pf} = f_{pe} + \Delta f_{pf} = f_{pe} + \Omega_u E_{pf} \varepsilon_{cc} \left(\frac{d_p - c}{c} \right) \quad (3)$$

where

f_{pe} = effective stress in prestressing steel at the section under consideration after all losses

Ω_u = strain reduction factor

E_{pf} = prestressing CFRP tendon elastic modulus

ε_{cc} = concrete compressive strain

d_p = depth of the tendon from the extreme compression fiber

c = distance from the extreme compression fiber to the neutral axis

The recommended strain reduction factor Ω_u can be calculated by Eq. (4) for one-point loading and Eq. (5) for third-point or uniform loading.

$$\Omega_u = \frac{1.5}{\left(\frac{L}{d_p} \right)} \quad \text{(one-point loading)} \quad (4)$$

$$\Omega_u = \frac{3.0}{\left(\frac{L}{d_p} \right)} \quad \text{(third-point or uniform loading)} \quad (5)$$

where

L = length of the tendon between the anchorages

The AASHTO LRFD specifications recommend Eq. (6), a simplified equation for calculating the stress at the ultimate state f_{ps} for unbonded prestressing steel tendons.

$$f_{ps} = f_{pe} + 900 \left(\frac{d_p - c}{\ell_e} \right) \leq f_{py} \quad (6)$$

where

ℓ_e = effective tendon length = $\dfrac{\ell_i}{1 + \left(N_s / 2 \right)}$

f_{py} = yield strength of prestressing steel

ℓ_i = length of tendon between anchorages

N_s = number of support hinges crossed by the tendon between anchorages or discretely bonded points

Eq. (6) is modified as Eq. (7) to account for the prestressing CFRP properties and presented for the simply supported beams.

$$f_{pf} = f_{pe} + \left(\frac{900}{n} \right) \left(\frac{d_p - c}{L} \right) \leq f_{pu} \quad (7)$$

where

n = modular ratio = E_s/E_{pf}

f_{pu} = ultimate tensile strength of the CFRP tendon

E_s = prestressing steel elastic modulus

Figure 14 plots the experimentally obtained moment capacities against the predicted capacities from the analytical procedures. For bonded post-tensioned beams, the predicted values from both ACI 440-4R and the AASHTO LRFD specifications showed a good correlation with the experimental results. However, for the unbonded beams, the values predicted based on ACI 440-4R were better correlated with the experimental results. Generally, predictions based on the AASHTO LRFD specifications were conservative. The ACI 440-4R model was adopted in the AASHTO *Guide Specifications for the Design of Concrete Bridge Beams Prestressed with Carbon Fiber-Reinforced Polymer (CFRP) Systems*.[40]

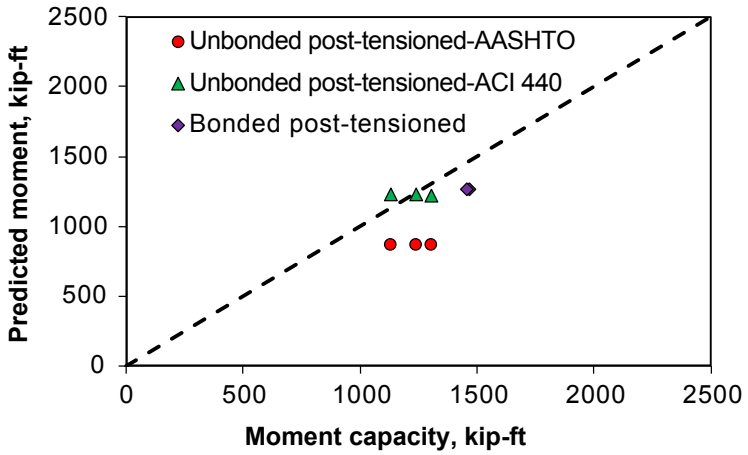

Figure 14. Experimental capacities versus the predicted values for post-tensioned concrete beams with carbon-fiber-reinforced polymer cables. Note: 1 kip-ft = 1.356 kN-m.

Conclusions

This paper presents the results of experiments on five full-scale beams post-tensioned with prestressing CFRP tendons and tested under monotonic and fatigue loading. The main findings include the following:

- The flexural capacity of bonded beams with prestressing CFRP was 20% higher than the flexural capacity of the unbonded post-tensioned beams.
- The CFRP-prestressed beams showed significant deformability before failure, and the deformability of the unbonded beams was 10% to 130% greater than the deformability of the bonded counterparts.
- The bonded and unbonded beams showed distinctly different crack patterns. The unbonded post-tensioned beams showed a few concentrated wide cracks whereas cracking in the bonded beams spread over almost the entire beam length.
- The 2.3 million load cycles in fatigue tests did not affect the stiffness or anchorage performance of the CFRP-prestressed beams.
- The procedures adopted by ACI 440-4R to predict the flexural moment capacity of bonded and unbonded post-tensioned beams correlated well with the test results.

Acknowledgments

This research project was funded by the National Cooperative Highway Research program (NCHRP) under the project NCHRP 12-97. The views expressed in this paper are those of the authors and do not necessarily reflect those of the funding agency.

References

1. Khalifa, M. A., S. S. Kuska, and J. Krieger. 1993. "Bridges Constructed Using Fiber Reinforced Plastics." *Concrete International* 15 (6): 43-47.
2. American Concrete Institute (ACI). 2011. *Prestressing Concrete Structures with FRP Tendons (Reapproved)*. ACI 440.4R-04. Farmington Hills, MI: ACI.
3. Abdelrahman, A. A., and S. H. Rizkalla. 1997. "Serviceability of Concrete Beams Prestressed by Carbon." *ACI Structural Journal* 94 (4): 447-457.
4. Kato, T., and N. Hayashida. 1993. "Flexural Characteristics of Prestressed Concrete Beams with CFRP Tendons." Proceedings, *International Symposium on Fiber-Reinforced-Plastic Reinforcement for Concrete Structures. ACI Symposium Papers* 138: 419-440. https://doi.org/10.14359/10036.
5. Lee, C., S. Shin, and H. Lee. 2017. "Balanced Ratio of Concrete Beams Internally Prestressed with Unbonded CFRP Tendons." *International Journal of Concrete Structures and Materials* 11 (1): 1-16.
6. Kakizawa, T., S. Ohno, and T. Yonezawa. 1993. "Flexural Behavior and Energy Absorption of Carbon FRP Reinforced Concrete Beams." Proceedings, International Symposium on Fiber-Reinforced-Plastic Reinforcement for Concrete Structures. ACI *Symposium Papers* 138: 585-598. https://doi.org/10.14359/3940.
7. Maissen, A., and C. A. M. De Smet. 1995. "Comparison of Concrete Beams Prestressed with Carbon Fibre Reinforced Plastic and Steel Strands." In *Non-metallic (FRP) Reinforcement for Concrete Structures:*

Proceedings of the Second International RILEM Symposium (FRPRCS-2), Ghent, 23-25 August 1995, edited by L. Taerwe, 430-439. London, U.K.: Taylor and Francis. https://doi.org/10.1201/9781482271621.

8. Maissen, A., and C. A. M. De Smet. 1998. "Prestressed Concrete Using Carbon Fibre Reinforced Plastic (CFRP) Strands." *Materials and Structures* 31 (3): 175-177. https://doi.org/10.1007/BF02480393.

9. Jo, B. W., G. H. Tae, and B. Y. Kwon. 2004. "Ductility Evaluation of Prestressed Concrete Beams with CFRP Tendons." *Journal of Reinforced Plastics and Composites* 23 (8): 843-859. https://doi.org/10.1177/0731684404033492.

10. Heo, S., S. Shin, and C. Lee. 2013. "Flexural Behavior of Concrete Beams Internally Prestressed with Unbonded Carbon-Fiber-Reinforced Polymer Tendons." *Journal of Composites for Construction* 17 (2), 167-175. https://doi.org/10.1061/(ASCE)CC.1943-5614.0000306.

11. Burke, C.R., and C. W. Dolan. 2001. "Flexural Design of Prestressed Concrete Beams Using FRP Tendons." *PCI Journal* 46 (2): 76-87. https://doi.org/10.15554/pcij.03012001.76.87.

12. Grace, N. F., B. M. Tang, and G. A. Sayed. 2001. "New Approach to Multi-span CFRP Continuous Prestressed Bridges." In *FRP Composites in Civil Engineering : Proceedings of the International Conference on FRP Composites in Civil Engineering, 12-15 December 2001, Hong Kong, China*, 1177-1184. Amsterdam, Netherlands: Elsevier.

13. Selvachandran, P., S. Anandakumar, and K. L. Muthuramu. 2017. "Influence of Deformability Behavior in Prestressed Concrete Beams Using Carbon-Fiber-Reinforced Polymer Tendon." *PCI Journal* 62 (1): 66-77. https://doi.org/10.15554/pcij62.1-04.

14. Grace, N. F., M .E. Mohamed, M. Kasabasic, M. Chynoweth, K. Ushijima, and M. Bebawy. 2022. "Design, Construction, and Monitoring of US Longest Highway Bridge Span Prestressed with CFRP Strands." *Journal of Bridge Engineering* 27 (7): 04022047. https://doi.org/10.1061/(ASCE)BE.1943-5592.0001881.

15. Dolan, C. W., H. R. Hamilton, C. E. Bakis, and A. Nanni. 2000. *Design Recommendations for Concrete Structures Prestressed with FRP Tendons, Final Report*. Federal Highway Administration (FHWA) Contract DTFH61-96-C- 00019. Washington, DC: FHWA. https://rosap.ntl.bts.gov/view/dot/50274.

16. Mertol, H. C., S. Rizkalla, P. Scott, J. M. Lees, and R. El-Hacha. 2006. "Durability and Fatigue Behavior of High-Strength Concrete Beams Prestressed with CFRP Bars." Proceedings, International Symposium on Case Histories and Use of FRP for Prestressing Applications. ACI *Symposium Papers* 245: 1-20. https://doi.org/10.14359/18759.

17. Braimah, A., M. F. Green, and T. I. Campbell. 2006. "Fatigue Behaviour of Concrete Beams Post-Tensioned with Unbonded Carbon Fibre Reinforced Polymer Tendons." *Canadian Journal of Civil Engineering* 33 (9): 1140-1155. https://doi.org/10.1139/l06-063.

18. Mutsuyoshi, H., and A. Machida. 1993. "Behavior of Prestressed Concrete Beams Using FRP as External Cable." Proceedings, International Symposium on FRP Reinforcement for Concrete Structures. ACI *Symposium Papers* 138: 401-418. https://doi.org/10.14359/3932.

19. Grace, N. F., and G. Abdel-Sayed. 1998. "Behavior of Externally Draped CFRP Tendons in Prestressed Concrete Bridges." *PCI Journal* 43 (5): 88-101. https://doi.org/10.15554/pcij.09011998.88.101.

20. Elrefai, A., J. S. West, and K. Soudki. 2007. "Performance of CFRP Tendon–Anchor Assembly under Fatigue Loading." *Composite Structures* 80 (3): 352-360. https://doi.org/10.1016/j.compstruct.2006.05.023.

21. Du, J. S., and F. T. K. Au. 2009. "Estimation of Ultimate Stress in External FRP Tendons." *Proceedings of the Institution of Civil Engineers—Structures and Buildings* 162 (4): 213-220. https://doi.org/10.1680/stbu.2009.162.4.213.

22. Ghallab, A. 2013. "Calculating Ultimate Tendon Stress in Externally Prestressed Continuous Concrete Beams Using Simplified Formulas." *Engineering Structures*, 46: 417-430. https://doi.org/10.1016/j.engstruct.2012.07.018.

23. Campbell, I. 2008. *Prestressing Concrete Structures with FRPs*. SimTREC Design Manual No. 5. Winnipeg, MB: Structural Innovation and Monitoring Technologies Resource Centre (SimTREC).

24. Canadian Standards Association. 2019. *Canadian Highway Bridge Design Code*. CAN/CSA-S6. Toronto, ON: CSA Group.

25. Naaman, A. E., and S. M. Jeong. 1995. "Structural Ductility of Beams Prestressed with FRP Tendons." In *Non-metallic (FRP) Reinforcement for Concrete Structures: Proceedings of the Second International RILEM Symposium (FRPRCS-2), Ghent, 23-25 August 1995,* edited by L. Taerwe, 379-386. London, U.K.: Taylor and Francis. https://doi.org/10.1201/9781482271621.

26. Abdelrahman, A. A., G. Tadros, and S. H. Rizkalla. 1995. "Test Model for First Canadian Smart Highway Bridge."

Structural Journal 92 (4): 451-458. https://doi.org/10.14359/994.

27. Zou, P. X. 2003. "Flexural Behavior and Deformability of Fiber Reinforced Polymer Prestressed Concrete Beams." *Journal of Composites for Construction* 7 (4): 275-284. https://doi.org/10.1061/(ASCE)1090-0268(2003)7:4(275).

28. Belarbi, A., M. Dawood, P. Poudel, M. Reda, H. Tahsiri, B. Gencturk, S. H. Rizkalla, and H. G. Russell. 2019. *Design of Concrete Bridge Beams Prestressed with CFRP Systems*. NCHRP (National Cooperative Highway Research Program) Report 907. Washington, DC: National Academies Press. https://dx.doi.org/10.17226/25582.

29. Poudel, P., A. Belarbi, B. Gencturk, and M. Dawood. 2022. "Flexural Behavior of Full-Scale, Carbon-Fiber-Reinforced Polymer Prestressed Concrete Beams." *PCI Journal* 67 (5): 22-39. https://doi.org/10.15554/pcij67.5-01.

30. ASTM International. 2015. *Standard Practice for Making and Curing Concrete Test Specimens in the Field*. ASTM C31/C31M-15. West Conshohocken, PA: ASTM International.

31. ASTM International. 2015. *Standard Test Method for Compressive Strength of Cylindrical Concrete Specimens*. ASTM C39/C39M-15. West Conshohocken, PA: ASTM International.

32. ASTM International.2011. *Standard Test Method for Tensile Properties of Fiber Reinforced Polymer Matrix Composite Bars*. ASTM D7205/D7205M-06(2011). West Conshohocken, PA: ASTM International.

33. ASTM International. 2006. *Standard Practice for Evaluating Material Property Characteristic Values for Polymeric Composites for Civil Engineering Structural Application*s. ASTM D7290-06. West Conshohocken, PA: ASTM International.

34. Mattock, A. H., J. Yamazaki, and B. T. Kattula. 1971. "Comparative Study of Prestressed Concrete Beams, with and without Bond." ACI *Journal Proceedings* 68 (2): 116-125. https://doi.org/10.14359/11298.

35. American Association of State Highway and Transportation Officials (AASHTO). 2020. *AASHTO LRFD Bridge Design Specifications*. 9th ed. Washington, DC: AASHTO.

36. Naaman A. E., and F. M. Alkhairi. 1991. "Stress at Ultimate in Unbonded Post-Tensioning Tendons: Part 2—Proposed Methodology." *Structural Journal* 88 (6): 683–692. https://doi.org/10.14359/1288.

37. MacGregor, R. J. G. 1989. "Strength and Ductility of Externally Post-Tensioned Segmental Box Girders," PhD diss., University of Texas at Austin.

38. Naaman, A. E., N. Burns, C. French, W. L. Gamble, and A. H. Mattock. 2002. "Stresses in Unbonded Prestressing Tendons at Ultimate: Recommendation." *Structural Journal* 99 (4): 518-529. https://doi.org/10.14359/12121.

39. Harajli, M. H. 2011. "Proposed Modification of AASHTO-LRFD for Computing Stress in Unbonded Tendons at Ultimate." *Journal of Bridge Engineering* 16 (6): 828-838. https://doi.org/10.1061/(ASCE)BE.1943-5592.0000183.

40. AASHTO. 2018. *Guide Specifications for the Design of Concrete Bridge Beams Prestressed with Carbon Fiber-Reinforced Polymer (CFRP) Systems*. Washington, DC: AASHTO.

Notation

a/d = shear span-to-depth ratio

c = distance from the extreme compression fiber to the neutral axis

d_p = depth of the tendon from the extreme compression fiber

E_{ela} = elastic energy, which is a part of the total energy

E_{pf} = prestressing carbon-fiber-reinforced polymer tendon elastic modulus

E_s = prestressing steel elastic modulus

E_{tot} = total energy under the load-deflection curve

f_{pe} = effective stress in prestressing steel at the section under consideration after all losses

f_{pf} = total force in the unbonded tendon

f_{ps} = stress at the ultimate state

f_{pu} = ultimate tensile strength of the carbon-fiber-reinforced polymer tendon

f_{py} = yield strength of prestressing steel

GDF = girder distribution factor

ℓ_e = effective tendon length

ℓ_i = length of tendon between anchorages

L = length of the tendon between the anchorages

n = modular ratio

N_s = number of support hinges crossed by the tendon between anchorages or discretely bonded points

P = load

α_1 = rectangular stress block parameter multiplying concrete strength

β_1 = rectangular stress block parameter multiplying neutral axis depth

ε_{cc} = concrete compressive strain

Δ_ℓ = equivalent deflection of an uncracked section at the same ultimate load

Δ_u = deflection at ultimate load

μ = deformability of CFRP-prestressed beams

μ_{en} = ductility index

Ω_u = strain reduction factor

Mahmoud R. Manaa, PhD, PE, is a bridge engineer with Jacobs in Houston, Texas. He received his bachelor's degree and master's degrees from Cairo University, Egypt, and his PhD from the University of Houston in Texas.

Abdeldjelil Belarbi, PhD, PE, is the Hugh Roy and Lillie Cranz Cullen Distinguished Professor at the University of Houston. His primary research focuses on the constitutive modeling of structural concrete and the use and design of innovative and advanced materials for new construction and strengthening of deteriorated civil engineering infrastructure.

Bora Gencturk, PhD, PE, is a professor in the Sonny Astani Department of Civil and Environmental Engineering at the University of Southern California, Los Angeles, California. He received his master's degrees and his PhD from the University of Illinois at Urbana-Champaign. His research focuses on the durability and extreme event resilience of reinforced concrete structures with emphasis on application of high-performance materials

Mina Dawood, PhD, was an associate professor at the University of Houston in Texas during the course of this research. His research focused on the application of new and advanced materials including carbon-fiber-reinforced polymer, ultra-high-performance concrete and shape memory alloy in structural applications for both new construction and rehabilitation of existing structures.

Abstract

This article reports on an investigation of the flexural behavior of post-tensioned composite AASHTO beams under flexural monotonic and fatigue loading. Five 39.5-ft-long (12-m) post-tensioned beams with 0.76-in.-diameter (19-mm) prestressing carbon-fiber-reinforced polymer (CFRP) cables were studied. Three beams were post-tensioned with unbonded cables, and the other two beams were post-tensioned with bonded cables. The fatigue resistance and the effect of tendon profile (straight versus draped) were investigated. The results showed that the two beams with unbonded tendons survived 2.3 million fatigue cycles with an insignificant effect on the deformation and stiffness of the beams. At the ultimate load, the beams with unbonded cables showed greater deformation compared with the counterparts with bonded cables; however, the flexural capacity of the unbonded beams was lower. Different analytical models for estimating the flexural capacity of the beams were assessed against the experimental results to determine the applicability of these models to full-scale CFRP post-tensioned beams.

Keywords

AASHTO beams, carbon-fiber-reinforced polymer, fatigue, flexure, post-tensioning, prestressed concrete.

Review policy

This paper was reviewed in accordance with the Precast/Prestressed Concrete Institute's peer-review process. The Precast/Prestressed Concrete Institute is not responsible for statements made by authors of papers in PCI Journal. No payment is offered.

Publishing details

This paper appears in *PCI Journal* (ISSN 0887-9672) V. 69, No. 1, January-February 2024, and can be found at https://doi.org/10.15554/pcij69.1-03. *PCI Journal* is published bimonthly by the Precast/Prestressed Concrete Institute, 8770 W. Bryn Mawr Ave., Suite 1150, Chicago, IL 60631.

Reader comments

Please address any reader comments to *PCI Journal* editor-in-chief Tom Klemens at tklemens@pci.org or Precast/Prestressed Concrete Institute, c/o PCI Journal, 8770 W. Bryn Mawr Ave., Suite 1150, Chicago, IL 60631.